POLITECNICO DI TORINO Repository ISTITUZIONALE

Power losses in thick steel laminations with hysteresis

Original Power losses in thick steel laminations with hysteresis / C., Appino; G., Bertotti; O., Bottauscio; F., Fiorillo; P., Tiberto; D., Binesti; J. P., Ducreux; Chiampi, Mario; Repetto, Maurizio In: JOURNAL OF APPLIED PHYSICS ISSN 0021-8979 79:(1996), pp. 4575-4577. [10.1063/1.361873]
Availability: This version is available at: 11583/1641889 since:
Publisher: AIP
Published DOI:10.1063/1.361873
Terms of use:
This article is made available under terms and conditions as specified in the corresponding bibliographic description in the repository
Publisher copyright

(Article begins on next page)

Power losses in thick steel laminations with hysteresis

C. Appino, G. Bertotti, O. Bottauscio, F. Fiorillo, and P. Tiberto Istituto Elettrotecnico Nazionale Galileo Ferraris, C. so M. d'Azeglio 42, 10125 Torino, Italy

D. Binesti and J. P. Ducreux

Electricité de France, DER, Les Renardières BP 1, 77250 Moret-sur-Loing, France

M. Chiampi and M. Repetto

Politecnico di Torino, C. so Duca degli Abruzzo 44, 10129 Torino, Italy

Magnetic power losses have been experimentally investigated and theoretically predicted over a range of frequencies (direct current—1.5 kHz) and peak inductions (0.5–1.5 T) in 1-mm-thick FeSi 2 wt. % laminations. The direct current hysteresis properties of the system are described by the Preisach model, with the Preisach distribution function reconstructed from the measurement of the recoil magnetization curve (B_p =1.7 T). On this basis, the time behavior of the magnetic induction vs frequency at different lamination depths is calculated by a finite element method numerical solution of Maxwell equations, which takes explicitly into account the Preisach model hysteretic B(H) relationship. The computed loop shapes are, in general, in good agreement with the measured ones. The power loss dependence on frequency is predicted and experimentally found to change from a $\sim f^{3/2}$ to a $\sim f^2$ law with increasing peak induction. © 1996 American Institute of Physics. [S0021-8979(96)36208-9]

I. INTRODUCTION

Power loss phenomena in soft magnetic laminations can be understood and assessed to a good extent through the statistical description of domain wall dynamics and the related development of new concepts in the Preisach modeling of hysteresis. Several interesting problems arise when this interpretative framework is applied to bulk materials and the related skin effects. In fact, one has to properly characterize the hysteretic magnetic behavior of the sheet, solve Maxwell equations in the presence of hysteresis, and carry out convenient dynamic hysteresis measurements in order to appropriately test the model predictions.

In this article, we study the dynamic behavior of 1-mm-thick FeSi sheets, for frequencies from direct current (dc) to 1.5 kHz and peak inductions in the interval from 0.5 to 1.5 T. The material hysteresis properties are described by the Preisach model (PM), and Maxwell equations are solved by the finite element method (FEM), and by using the fixed point (FP) technique to treat the nonlinear hysteretic behavior of the material. This requires the use of PM in a reversed fashion, in order to obtain, at each iteration step, the time behavior of the local field **H** from the known local induction wave form.³ From the knowledge of the magnetic flux density distribution, the dynamic hysteresis loops and the local losses at different frequencies can be calculated.

We have found that the calculated loop shapes are in general in good agreement with the measured ones. At low peak inductions B_p , the skin effect prevents the complete flux penetration in the sheet and the power loss dependence on frequency is close to a $f^{3/2}$ law. With increasing B_p , however, the skin effect is no longer able to hinder the flux penetration and a complicated phase shift pattern in the flux densities at different lamination depths sets in. In this case the power loss vs frequency law moves to a f^2 law.

The present approach does not take into account magnetic domain effects responsible for excess losses. This as-

pect could be dealt with by using the dynamic Preisach model instead of the conventional one. 1,4

II. THEORETICAL MODELING

Calculations were based on the standard FEM solution of Maxwell equations expressed in term of the vector potential **A**. The starting point is the equation

$$\nabla \times [H(\nabla \times \mathbf{A})] = -\sigma \frac{\partial \mathbf{A}}{\partial t} + \frac{\sigma}{S} \int_{\Omega} \frac{\partial \mathbf{A}}{\partial t} dS', \tag{1}$$

together with nonhomogeneous Dirichlet conditions, which impose the stated flux wave form. In Eq. (1), σ is the electric conductivity and Ω is the cross section of the lamination with area S. We assumed the local \mathbf{H} and \mathbf{B} vectors to always be collinear, and a scalar treatment of the $\mathbf{H}(\mathbf{B})$ relation was considered. Following the fixed point (FP) technique, the relation between \mathbf{H} and \mathbf{B} is expressed as $\mathbf{H}(\mathbf{B}) = \nu_T \mathbf{B} + \mathbf{R}$. The coefficient ν_T is related to the slope of the initial magnetization curve and is held constant throughout the calculation. The residual term \mathbf{R} is iteratively evaluated, starting from a trial value.

Under periodic conditions, the problem is formulated in the frequency domain, introducing a set of complex vector potential harmonics $\mathbf{A}^{(n)}$, where n is the harmonic order corresponding to the angular frequency $n\omega$. The application of the iterative FP scheme to Eq. (1) leads to a sequence of linear problems, having the form

$$\nabla \times (\nu_T \nabla \times \mathbf{A}_k^{(n)}) = -i \omega n \, \sigma \mathbf{A}_k^{(n)} + i \omega n \, \frac{\sigma}{S} \, \int_{\Omega} \mathbf{A}_k^{(n)} \, dS'$$
$$- \nabla \times \mathbf{R}_{k-1}^{(n)}, \qquad (2)$$

where k is the iteration index. The problem is unidimensional, since any quantity depends only on the depth x across the lamination thickness. Following FEM, the lamination is subdivided into a conveniently high number (\sim 100) of lay-

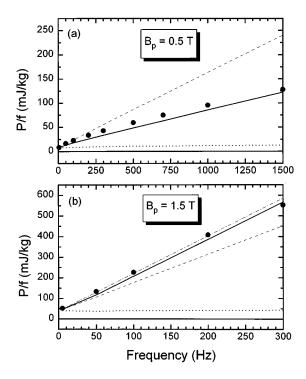


FIG. 1. (a) Energy loss vs frequency at B_p =0.5 T. Points: experiments; dotted line: computed hysteresis loss; continuous line: computed total loss; dashed line: total loss obtained by adding to the hysteresis loss the standard classical expression holding in the absence of skin effect. (b) Same for B_p =1.5 T. Dash-dotted line: analytical prediction obtained by assuming $B = +B_p$ when H > 0, $B = -B_p$ when H < 0.

ers and on each layer the solution is interpolated by means of first order shape functions. It is worth noting that the FP iterations change only the right-hand side of Eq. (2), without requiring any modification of the stiffness matrix.

At each iteration step, all the harmonic components of the vector potential \mathbf{A} are calculated, providing the corresponding components of the magnetic induction $\mathbf{B} = \nabla \times \mathbf{A}$. The time behavior of \mathbf{B} is obtained by an inverse fast Fourier transform of the harmonic components. The $\mathbf{H}(\mathbf{B})$ dependence is described through PM, used in a reversed fashion, in order to compute the local field wave form $\mathbf{H}(\mathbf{t})$ that generates the known local \mathbf{B} wave form. Once the \mathbf{B} and \mathbf{H} wave forms are known, the time evolution of the residue \mathbf{R}_k is computed over each element, the harmonic decomposition is performed again and the right-hand side of Eq. (2) is upgraded. The computation scheme is iterated until convergence.

For any given solution, the total loss was calculated by taking the time integral of the field at the lamination surface times the mean induction rate, i.e., averaged over all mesh elements. The hysteresis loss was instead calculated by taking the time integral of \mathbf{H} d \mathbf{B} in each mesh element and integrating the result over the whole lamination volume. Classical losses can be also evaluated by integrating the quantity J^2/σ in space and time, where the current density \mathbf{J} is evaluated from the vector potential \mathbf{A} . The comparison between the total loss and the sum of the hysteresis and classical losses provided an additional check of the computation accuracy.

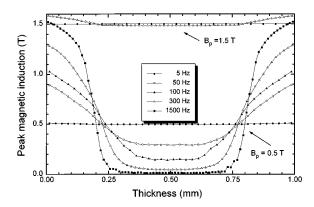


FIG. 2. Computed profiles of the peak induction vs lamination depth at different exciting frequencies for macroscopic peak induction B_p =0.5 and 1.5 T.

The switching field Preisach distribution used to characterize the material was assumed to have the factorized form $p(\alpha,\beta)=f(\alpha)f(-\beta)$, which is the natural factorization expected in soft magnetic laminations. $p(\alpha,\beta)$ was reconstructed, as suggested in Ref. 6, from the recoil curve of the loop measured at peak induction $p(\alpha,\beta)$ was found to be sharply peaked at low $p(\alpha,\beta)$ values, as expected from the shape of the experimentally determined static hysteresis loops. In order to efficiently handle the numerical problem, the Preisach plane was covered with a mesh having increased density in the region where the peak of $p(\alpha,\beta)$ was located.

III. EXPERIMENTAL RESULTS AND DISCUSSION

Dynamic hysteresis loops and power losses were measured by a digital feedback wattmeter which allows one to carry out measurements under controlled induction wave form in a wide frequency range (0.5 Hz–100 kHz).⁷ Static hysteresis loops and the normal magnetization curve were determined by means of a precision ballistic setup. Experiments were performed on 2 wt % Si–Fe alloys. Laminations 1 mm thick were tested as 30×300 mm strips, inserted in an Epstein frame with a reduced number of turns.

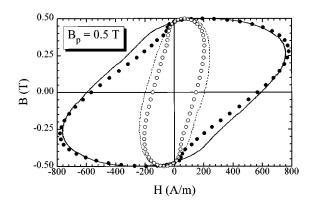


FIG. 3. Experimental and computed hysteresis loops for B_p =0.5 T. Lines: measurements (dashed: f=300 Hz, continuous; f=1.5 kHz). Symbols: theoretical prediction.

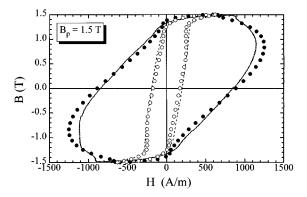


FIG. 4. Instantaneous profiles of the induction B(x) at different times t along the period T, at t = 300 Hz and macroscopic peak induction $B_p = 1.5$ T. A: t = 0; B: t = T/8; C: t = T/4; D: t = 3T/8; E: t = T/2.

The loss per cycle vs frequency at 0.5 T is shown in Fig. 1(a). The continuous line represents the FEM calculated total loss, while the dotted line is the hysteresis loss, obtained from the integral of local H dB over time and over the mesh elements. The calculations show that the hysteresis loss, which would be independent of f in the absence of any skin effect, increases with frequency, because of the nonconstant peak induction profile vs lamination depth. The dashed line represents the sum of the hysteresis loss and the standard classical loss $P_c/f = (\pi^2/6)\sigma d^2 B_p^2 f/\delta$ (d is the lamination thickness and δ is the mass density). As expected, this law gives a grossly overestimated total loss figure in the frequency range where the skin effect becomes important. This is well illustrated by Fig. 2, which shows the FEM calculated frequency dependence of the peak induction profiles vs lamination depth. Above a few hundred Hz, about half of the lamination becomes flux depleted, an effect compensated by the strong increase of $B_p(x)$ near the surface. The measured and calculated hysteresis loops at 300 Hz and 1.5 kHz are shown in Fig. 3. At low f, some disagreement between the predicted and measured loop shapes was found. This is likely due to limitations in the identification of the Preisach distribution, which was based on data at 1.7 T only.

The loss behavior at 1.5 T shows that, with the increase of the macroscopic peak induction, the slope of the experimental P/f vs f curve suffers a progressive increase, which is correctly predicted by the model [see Fig. 1(b), and Fig. 4 for the loop shapes]. The loss values obtained by both measurements and FEM calculations are larger than the ones calculated through the standard classical loss expression given above, just the opposite of what was observed at 0.5 T. This difference is the consequence of the qualitatively different flux penetration pattern in the lamination. As shown in Fig. 2, the peak induction attains quite a uniform profile over the lamination cross section. But such a peak value is reached at different times for different depths (see Fig. 5) and it is this phase difference that causes additional inhomogeneities in the magnetization rate spatial distribution and ensu-

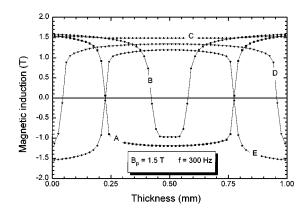


FIG. 5. Experimental and computed hysteresis loops for B_p =1.5 T. Lines: measurements (dashed: f=50 Hz, continuous; f=300 kHz). Symbols: theoretical prediction.

ing higher losses. Some useful information on this behavior can be obtained analytically, without resorting to FEM calculations. In fact, when B_p is comparable with the saturation magnetization and the dynamic fields involved in the problem are much larger than the material coercivity, the **B(H)** relation can be approximated by a step function of the form $B = +B_p$ when H > 0, $B = -B_p$ when H < 0. In this case, the flux and field distribution inside the lamination can be calculated analytically, and the loss turns out to be equal to $(4/3)P_c$, where P_c is the standard expression given above.

IV. CONCLUSIONS

The present calculations predict hysteresis and classical losses, but not excess losses due to magnetic domain effects. From the quantitative point of view, this is not expected to lead to important errors in the steel here considered, where the excess loss plays a minor role due to the fine grain size, but it might become relevant for those laminations where the grain size exceeds values of the order of 100 μ m. In cases of interest, one can include domain effects into the treatment by considering the so-called dynamic Preisach model, as recently proposed by some authors.⁴ This model is equivalent to introducing a local **B(H)** relationship which depends not only on the **H** history, but also on the field rate $d\mathbf{H}/dt$. The use of the dynamic Preisach model would not require any substantial change in the design of the FEM algorithm presented here. The main difference is likely to be the drastic increase of the computation time, as a consequence of the complex internal structure of the dynamic Preisach model.

¹G. Bertotti and M. Pasquale, IEEE Trans. Magn. 28, 2787 (1992).

²R. M. Del Vecchio, J. Appl. Phys. **53**, 8281 (1982).

³O. Bottauscio, M. Chiampi, D. Chiarabaglio, and M. Repetto, IEEE Trans. Magn. 31, 3548 (1995).

⁴D. A. Philips, L. R. Dupre, and J. A. A. Melkebeek, IEEE Trans. Magn. 30, 4377 (1994).

⁵V. Basso, M. Lo Bue, and G. Bertotti, J. Appl. Phys. **75**, 5677 (1994).

⁶G. Kadar, J. Appl. Phys. **61**, 4013 (1987).

⁷G. Bertotti, E. Ferrara, F. Fiorillo, and M. Pasquale, J. Appl. Phys. **73**, 5375 (1993).